Pharmaceutical Research, Vol. 25, No. 1, January 2008 (© 2007)
DOI: 10.1007/s11095-007-9451-9

Research Paper

Paclitaxel Prodrugs with Sustained Release and High Solubility in Poly(ethylene glycol)-*b*-poly(ε-caprolactone) Micelle Nanocarriers: Pharmacokinetic Disposition, Tolerability, and Cytotoxicity

M. Laird Forrest,[1,4] Jaime A. Yáñez,[2] Connie M. Remsberg,[2] Yusuke Ohgami,[2] Glen S. Kwon,[3] and Neal M. Davies[2]

Received May 18, 2007; accepted August 29, 2007; published online October 3, 2007

Purpose. Develop a Cremophor® and solvent free formulation of paclitaxel using amphiphilic block copolymer micelles of poly(ethylene glycol)-*b*-poly(ε-caprolactone) (PEG-*b*-PCL) and characterize their release, solubility, cytotoxicity, tolerability, and disposition.
Methods. Hydrophobic prodrugs of paclitaxel were synthesized via DCC/DMAP or anhydride chemistry to overcome the poor loading (<1% *w/w*) of paclitaxel in micelles of PEG-*b*-PCL. Micelles were prepared by a co-solvent extraction technique. A micellar formulation of paclitaxel prodrug (PAX7′C_6) was dosed intravenously to rats (10 mg/kg) and compared to Taxol® (paclitaxel in CrEL:EtOH) and PAX7′C_6 in CrEL:EtOH as controls at the same dose. Pharmacokinetic parameters and tissue distribution were assessed.
Results. Paclitaxel prodrugs had solubilities >5 mg/ml in PEG-*b*-PCL micelles. Resulting PEG-*b*-PCL micelles contained 17-22% w/w prodrug and were less than 50 nm in diameter. PEG-*b*-PCL micelles released paclitaxel prodrugs over several days, $t_{1/2}$>3 d. Only the 7′derivative of paclitaxel with the shortest acylchain 7′hexonoate (PAX7′C_6) maintained cytotoxic activity similar to unmodified paclitaxel. PAX7′C_6 micelles demonstrated an increase in area under the curve, half-life, and mean residence time while total clearance and volume of distribution decreased.
Conclusions. Paclitaxel prodrugs in PEG-*b*-PCL micelle nanocarriers augment the disposition and increase tolerability making further studies on tumor efficacy warranted.

KEY WORDS: nanocarrier; paclitaxel; pharmacokinetics; polymer micelle; prodrug.

INTRODUCTION

Paclitaxel has demonstrated efficacy in the treatment of a variety of cancers [1–4]. However, the poor patient tolerability and life-threatening hypersensitivity reactions to the current Taxol® formulation (paclitaxel in Cremophor® EL: Ethanol—CrEL:EtOH) have driven development of safer, improved, and less antagonistic delivery systems. For instance, the Food and Drug Administration (FDA) has recently approved an albumin-coated nanoparticle paclitaxel formulation with decreased toxicity, but it has been reported that albumin nanoparticles are rapidly cleared by the mononuclear phagocyte system [5,6].

Amphiphilic block copolymer (ABC) micelles are an intriguing group of self-assembled nanocarriers for drug delivery, owing to the prospects of biocompatibility, large solubilization capacity for poorly water soluble molecules, and potential for passive drug targeting to solid tumors via the enhanced permeability and retention (EPR) effect [7]. Poly(ethylene glycol)-*block*-poly(ε-caprolactone) (PEG-*b*-PCL) copolymers are especially promising due to their kinetic and thermodynamic stability (critical micelle concentration typical <1 μM), biocompatibility, and both components (poly(ethylene glycol)—PEG and poly(ε-caprolactone)—PCL) are FDA approved for use in humans. The utilization of ABC micelles has been effective in encapsulating different lipophilic drug molecules without the inclusion of potentially harmful surfactants and excipients such as Cremophor® EL and ethanol [8–10].

Poly(ethylene glycol)-*block*-poly(ε-caprolactone) (PEG-*b*-PCL) copolymers have demonstrated sustained circulation

[1] College of Pharmacy, Department of Pharmaceutical Chemistry, The University of Kansas, Simons Labs, 2095 Constant Ave, Rm. 136B, Lawrence, Kansas 66047-3729, USA.
[2] Department of Pharmaceutical Sciences, College of Pharmacy, Washington State University, Pullman, Washington, USA.
[3] Division of Pharmaceutical Sciences, School of Pharmacy, University of Wisconsin-Madison, 777 Highland Avenue, Madison, Wisconsin 53705-2222, USA.
[4] To whom correspondence should be addressed. (e-mail: mforrest@ku.edu)

ABBREVIATIONS: $CDCl_3$, Deuterated Chloroform; CH_2Cl_2, Methylene chloride; CrEL, Cremophor EL; DMAP, 4-Dimethylaminopyridine; DMF, *N,N*-dimethylformamide; EtOAc, Ethyl acetate; EtOH, Ethanol; HCl, Hydrochloric acid; Na_2SO_4, Sodium sulfate; NH_4Cl, Ammonium chloride; PEG-*b*-PCL, Poly(ethylene glycol)-*b*-poly(ε-caprolactone); TBAF, Tetrabutylamoniumfloride; TBDMSCl, Tert-butyldimethylsilyl chloride; TBS, Tetrabromo-2-benzotriazole; THF, Tetrahydrofuran; TLC, Thin layer chromatography.

0724-8741/08/0100-0194/0

in rodents and biocompatibility [11]. PEG-*b*-PCL micelles are good candidates for poorly water soluble molecules in preclinical development, requiring drug solubilization, and optimized delivery. We have previously demonstrated that PEG-*b*-PCL can solubilize hydrophobic drugs such as amphotericin B, rapamycin, and geldanamycin prodrugs, owing to the highly hydrophobic nature of PCL [7–10,12,13]. However, they are unable to sufficiently solubilize paclitaxel, without extensive cross-linking of the core [14], which may incur manufacturing and regulatory issues.

We hypothesized that rendering paclitaxel more hydrophobic and bulky by the synthesis of acyl ester prodrugs of paclitaxel would increase the incorporation of the drug into PEG-*b*-PCL micelles and result in sustained release. This hypothesis emerges from an estimation of drug-PCL compatibility based on the Flory-Huggin drug-PCL parameter, often used to gauge polymer–solvent interaction [9,15].

The aims of these investigations are to overcome the solubilization problems of paclitaxel (Fig. 1, compound **1**) by synthesis and encapsulation of novel acyl ester prodrugs of paclitaxel. Subsequently, we determined the ability to retain *in vitro* anti-cancer activity and the pharmacokinetics and tissue distribution of the acyl ester prodrug of paclitaxel—PAX7′C_6 (Fig. 1, compound **4a**), our lead candidate, solubilized in PEG-*b*-PCL compared to Taxol® (paclitaxel in Cremophor CrEL: EtOH) and PAX7′C_6 (in CrEL:EtOH) as control formulations.

MATERIALS AND METHODS

Paclitaxel Prodrug Synthesis

Hydrophobic prodrugs of paclitaxel were synthesized according to the procedure of Ali and co-workers [16]. Briefly, paclitaxel was conjugated at the 2' and 7′ hydroxyl to fatty acids of increasing length (up to 16 carbons) via DCC/DMAP or anhydride chemistry [16] (Fig. 1). Synthesis of 6 derivatives of paclitaxel **1** was undertaken and included 7′hexonate-paclitaxel **4a**, 7′dodeconate-paclitaxel **4b**, 7′palmitate-paclitaxel **4c**, 2'hexonate-paclitaxel **5a**, 2'dodeconate-paclitaxel **5b**, and 2'palmitate-paclitaxel **5c** (Fig. 1). Examples of the synthesis procedures for 7′palmitate-paclitaxel **4c** and 2'palmitate-paclitaxel **5c** are given below.

Synthesis of 7-palmitate-paclitaxel 4c

The method for synthesis of 7-palmitate-paclitaxel **4c** is described below. Synthesis of **4a–b** were according to the same procedure, with substitution of the appropriate fatty anhydride.

2-TBS-paclitaxel 2. To a solution of paclitaxel **1** (300 mg, 0.35 mmol) in 1.2 ml dry DMF, TBDMSCl (158.84 mg, 1.053 mmol) and imidazole (59.80 mg, 0.8783 mmol) were added. The reaction mixture was stirred at room temperature for 12 h. The resulting solution was reduced to dryness in vaccuo, redissolved in 2 ml CH_2Cl_2, washed with saturated NH_4Cl (5 mlx/1) followed by water (5 ml × 1), and the organic layer dried over Na_2SO_4. Removal of the solvent followed by preparatory TLC on silica (1:1 EtOAc:hexane) provided **2** as a white solid (310.42 mg, 95% yield). ^{1}H NMR (400 MHz, $CDCl_3$) δ 0.5 (s, 9H, *tert*-butyl), 1.10 (s, 3H, H17), 1.22 (s, 3H, H16), 1.76 (s, 3H, H19), 1.93 (s, 3H, H18), 1.92–2.14 μm, 2H, H6), 2.3 and 2.56 (m, 2H, H14), 2.58 (s, 3H, 4-Ac), 3.91 (d, J = 6.9 Hz, 1H, H3), 4.23 (d, J = 8.1 Hz, 1H, H20), 4.30 (d, J = 1.8 Hz, 1H, 10-OH), 4.35 (d, J = 8.1 Hz, 1H, H20), 4.42 (dd, J = 6.6 and 10.8 Hz, 1H, H7), 4.68 (d, J = 2.1 Hz, 1H, H2'), 4.98 (dd, J = 1.5 and 9.3 Hz, 1H, H5), 5.13 (d, J = 1.8 Hz, 1H, H10), 5.69 (d, J = 6.9 Hz, 1H, H2), 5.73 (dd, J = 1.8 and 9 Hz, 1H, H3'), 6.34 (t, J = 8.7 Hz, 1H, H13), 7.11 (d, J = 9 Hz, 1H, NH), 7.33–8.16 (m, 15H).

2-TBS-7-palmitate-paclitaxel 3. To a solution of **2** (50 mg, 0.053 mmol) in 1 ml dry toluene, palmitic anhydride (38.3 mg, 0.0774 mmol) was added. The reaction mixture was stirred at 90°C for 18 h. The resulting solution was washed with 1-M HCl (5 ml × 1) followed by water (5 ml × 1), and the organic layer was dried over Na_2SO_4. Removal of the solvent followed by preparatory TLC on silica (1:1 EtOAc:hexane) provided **3** as a white solid (25 mg, 41% yield).

^{1}H NMR (400 MHz, $CDCl_3$) δ 0.5 (s, 9H, *tert*-butyl), 0.88 (t, 3H, CH_3), 1.10 (s, 3H, H17), 1.22 (s, 3H, H16), 1.76 (s, 3H, H19), 1.93 (s, 3H, H18), 1.92–2.14 (m, 2H, H6), 2.3 and 2.56 (m, 2H, H14), 2.58 (s, 3H, 4-Ac), 3.91 (d, J = 6.9 Hz, 1H, H3), 4.23 (d, J = 8.1 Hz, 1H, H20), 4.30 (d, J = 1.8 Hz, 1H, 10-OH), 4.35 (d, J = 8.1 Hz, 1H, H20), 4.42 (dd, J = 6.6 and 10.8 Hz, 1H, H7), 4.68 (d, J = 2.1 Hz, 1H, H2'), 4.98 (dd, J = 1.5 and 9.3 Hz, 1H, H5), 5.13 (d, J = 1.8 Hz, 1H, H10), 5.69 (d, J = 6.9 Hz, 1H, H2), 5.73 (dd, J = 1.8 and 9 Hz, 1H, H3'), 6.34

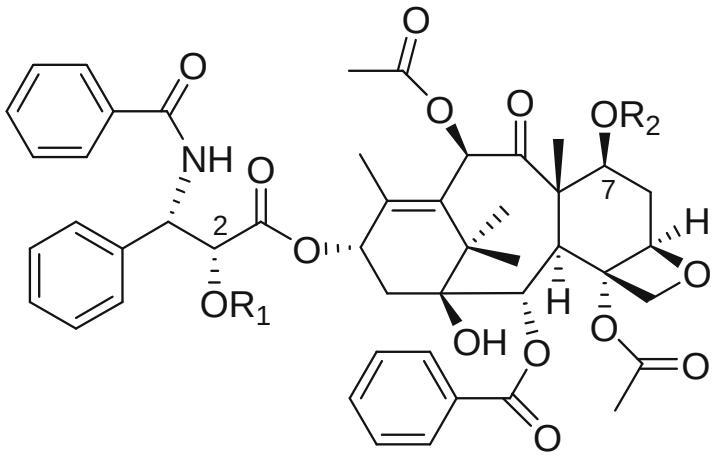

	R_1 (C_2)	R_2 (C_7)
1	H	H
2	Si(*tert*-butyl)	H
3	Si(*tert*-butyl)	$CO(CH_2)_{14}CH_3$
4a	H	$CO(CH_2)_4CH_3$
4b	H	$CO(CH_2)_{10}CH_3$
4c	H	$CO(CH_2)_{14}CH_3$
5a	$CO(CH_2)_4CH_3$	H
5b	$CO(CH_2)_{10}CH_3$	H
5c	$CO(CH_2)_{14}CH_3$	H

Fig. 1. Paclitaxel prodrug synthesis scheme.

(t, $J = 8.7$ Hz, 1H, H13), 7.11 (d, $J = 9$ Hz, 1H, NH), 7.33–8.16 (m, 15H).

7-palmitate-paclitaxel 4c. To a solution of **3** (25 mg, 0.211 mmol) in 1 ml of THF, 5 drops of 1-M TBAF (tetrabutylamoniumfloride) in THF was added. The reaction mixture was stirred at room temperature for 1 h. The resulting solution was reduced to dryness in vaccuo, redissolved in 2 ml CH_2Cl_2, washed with water (5 ml × 1), and the organic layer dried over Na_2SO_4. Removal of solvent followed by preparatory TLC on silica (1: 1 EtOAc:hexane) provided **4c** as a white solid (20 mg, 90% yield). ^{1}H NMR (400 MHz, $CDCl_3$) δ 0.88 (t, 3H, CH_3), 1.10 (s, 3H, H17), 1.22 (s, 3H, H16), 1.76 (s, 3H, H19), 1.93 (s, 3H, H18), 1.92–2.14 (m, 2H, H6), 2.3 and 2.56 (m, 2H, H14), 2.58 (s, 3H, 4-Ac), 3.91 (d, $J = 6.9$ Hz, 1H, H3), 4.23 (d, $J = 8.1$ Hz, 1H, H20), 4.30 (d, $J = 1.8$ Hz, 1H, 10-OH), 4.35 (d, $J = 8.1$ Hz, 1H, H20), 4.42 (dd, $J = 6.6$ and 10.8 Hz, 1H, H7), 4.68 (d, $J = 2.1$ Hz, 1H, H2'), 4.98 (dd, $J = 1.5$ and 9.3 Hz, 1H, H5), 5.13 (d, $J = 1.8$ Hz, 1H, H10), 5.69 (d, $J = 6.9$ Hz, 1H, H2), 5.73 (dd, $J = 1.8$ and 9 Hz, 1H, H3'), 6.34 (t, $J = 8.7$ Hz, 1H, H13), 7.11 (d, $J = 9$ Hz, 1H, NH), 7.33–8.16 (m, 15H).

Synthesis of 2-palmitate-paclitaxel 5c. The method for synthesis of 2-palmitate-paclitaxel **5c** is described below. Synthesis of **5a–b** were according to the same procedure, with substitution of the appropriate fatty anhydride.

2-palmitate-paclitaxel 5c. To a solution of paclitaxel **1** (100 mg, 0.117 mmol) in 1.5 ml dry toluene was added palmitic anhydride (115.79 mg, 0.234 mmol) and DMAP (11.435 mg, 0.0936 mmol). The reaction mixture was stirred at room temperature for 12 h. The resulting solution was washed with a 1-M HCl (5 ml × 1) and water (5 ml × 1), and the organic layer was dried over Na_2SO_4. Removal of solvent followed by preparatory TLC (1:1 EtOAc:hexane) provided **5c** as a white solid (60 mg, 47% yield). ^{1}H NMR (400 MHz, $CDCl_3$) δ 0.87 (t, 3H, CH_3), 1.10 (s, 3H, H17), 1.22 (s, 3H, H16), 1.76 (s, 3H, H19), 1.93 (s, 3H, H18), 1.92–2.14 (m, 2H, H6), 2.3 and 2.56 (m, 2H, H14), 2.58 (s, 3H, 4-Ac), 3.91 (d, $J = 6.9$ Hz, 1H, H3), 4.23 (d, $J = 8.1$ Hz, 1H, H20), 4.30 (d, $J = 1.8$ Hz, 1H, 10-OH), 4.35 (d, $J = 8.1$ Hz, 1H, H20), 4.42 (dd, $J = 6.6$ and 10.8 Hz, 1H, H7), 4.68 (d, $J = 2.1$ Hz, 1H, H2'), 4.98 (dd, $J = 1.5$ and 9.3 Hz, 1H, H5), 5.13 (d, $J = 1.8$ Hz, 1H, H10), 5.69 (d, $J = 6.9$ Hz, 1H, H2), 5.73 (dd, $J = 1.8$ and 9 Hz, 1H, H3'), 6.34 (t, $J = 8.7$ Hz, 1H, H13), 7.11 (d, $J = 9$ Hz, 1H, NH), 7.33–8.16 (m, 15H).

Preparation and Characterization of Prodrug Loaded PEG-*b*-PCL Micelles

Paclitaxel prodrug loaded PEG-*b*-PCL micelles were prepared by dissolving PEG-*b*-PCL (5000:10500, M_w/M_n 1.11, JCS Biopolytech Inc., Toronto, Ontario Canada) and prodrug in a minimum volume of acetone and adding drop-wise to vigorously stirred ddH_2O using a syringe pump. The organic solvent was then removed by stirring under an air purge. Where stated, samples were further concentrated by prolonged evaporation under an air purge. After removing the organic solvent, PEG-*b*-PCL micelles were passed through a 0.22-μm polyestersulfone filter to remove insoluble material and unincorporated drug [8]. In a typical experiment, 1 μM of PEG-*b*-PCL was dissolved in 0.75 ml of dry acetone and added dropwise (50 μl/min) to 2 ml of ddH_2O yielding 0.5-μM PEG-*b*-PCL micelles after removing the volatile organic solvent.

The incorporation of prodrugs into PEG-*b*-PCL micelles was verified by equivalent retention times in ultraviolet (UV) and refractive index (RI) chromatographs from gel permeation chromatography. PEG-*b*-PCL micelles were injected on an OHpak SB-806M GPC column (20-μl injections, 0.5-μM PEG-*b*-PCL, 0.75 ml/min of ddH_2O, 10°C; Shodex, Kawasaki, Japan) and detected by refractive index (RI) and UV absorbance (228 nm). Prodrug loading into PEG-*b*-PCL micelles was quantitatively determined by reverse-phase HPLC (Alltech Econosphere 3-μm 4.6 × 50 mm) using a 0.01% (*v*/*v*) trifluoroacetic acid (TFA)—acetonitrile (ACN) gradient (40–100% ACN, 50°C, 228-nm detection and trans-stilbene as internal standard). Hydrodynamic diameters of PEG-*b*-PCL micelles were determined by dynamic light scattering (DLS; NICOMP 380 ZLS, Particle Sizing Systems, Santa Barbara, CA). Data were analyzed by intensity-weighted Gaussian distribution fitting (NICOMP version 1.76). Measurements were made for a minimum of 10 min or at least 100×10^5 counts in channel 1.

PEG-*b*-PCL Micelle Prodrug Release Studies

Release experiments were based on the methodology of Eisenberg and coworkers [17] with modifications for temperature and pH control. Micelle prodrug solutions were prepared at 0.5 μM (PEG-*b*-PCL basis) with 20% *w*/*w* prodrug as above, and 0.5 ml of each solution was diluted to 2.5 ml with ddH_2O and injected into 10,000 MWCO dialysis cassettes (Pierce, Rockford, IL; $n = 4$). As a control, an equal quantity of prodrug dissolved in 100 μl of EtOH was injected into separate cassettes ($n = 3$). Dialysis cassettes were placed in a well-mixed temperature controlled water bath at 37°C, overflowed with ddH_2O so that the bath volume was refreshed every 15 to 20 min. Peristaltic pumps under computer control separately injected 50 g/l solutions of tribasic and monobasic phosphate to maintain pH at 7.4 ± 0.05 (apparatus built in-house). At fixed time points, dialysis cassette volumes were made up to 2.5 ml with ddH_2O, 100-μl aliquots l aliquots withdrawn, and prodrug concentrations determined by reverse-phase HPLC (see *supra*).

Octanol-Water Partition Coefficients

Octanol-water partition coefficients (log $P_{o/w}$) of paclitaxel prodrugs were determined indirectly by microemulsion electrokinetic chromatography (MEEKC) based on the technique of Klotz *et al.* [18]. Running buffer was prepared by titration of 25-mM sodium phosphate monobasic with 50-mM sodium tetraborate to pH 7.00, and 1.44 g of sodium dodecyl sulfate, 6.49 g of 1-butanol, and 0.82 g of heptane were made up to 100 ml with phosphate-borate buffer. The running buffer was ultrasonicated for 30 min in a closed 250-ml flask in ice water (G112SP1 Special Ultrasonic Cleaner, Laboratory Supplies Company Inc., Hicksville, NY). Longer times may be required to obtain a stable emulsion with lower power ultrasonicators. Compounds and standards ($n = 3$) were dissolved in the running buffer (0.05 mg/ml) with 0.5 μl/ml of nitromethane and 0.5 μl/ml of 1-phenyldodecane by ultrasonication (10 min) in a closed tube and centrifuged

(16,000×*g*, 3 min) to degas. A BioFocus 3000 capillary electrophoresis system (Bio-Rad, Hercules, CA) equipped with a 50-μm ID × 37-cm uncoated fused-silica column (Polymicron Technologies LLC, Phoenix, AZ) was used for MEEKC experiments. The column was prewashed with 1-M NaOH for 5 min and before runs with 0.1-M NaOH for 1 min, ddH_2O for 1 min, and running buffer for 1 min at 100 psi (690 kPa). Running conditions were 10 kV (ca. 30–35 μA, 30 min/run) at 20°C with 1-psi·s injections (6.9 kPa·s) and detection at 210 and 232 nm. Log $P_{o/w}$ and retention factors, k', were calculated using the equations:

$$\log P_{o/w} = a \cdot \log k' + b$$

$$k' = \frac{t_r - t_0}{t_0(1 - t_r/t_{me})}$$

where t_r, t_0, and t_{me} are retention times of the prodrug, nitromethane, and 1-phenyldodecane, respectively. Fitting parameters a and b were determined by linear regression of known standards: pyridine, phenol, benzoic acid, anisole, benzene, toluene, dodecanoic acid, benzopyrene, and pyrene ($R^2 = 0.996$, Excel® 2003, Microsoft Corp.).

Paclitaxel 7′C_6 (PAX7′C_6) Formulation in PEG-*b*-PCL Micelles

Paclitaxel 7′C_6 (PAX7′C_6) loaded PEG-*b*-PCL micelles were prepared as described above. The drug solution was made isotonic with 300 mg dextrose (5% *w*/*v*) and then filter-sterilized. The control formulations of paclitaxel in Cremophor CrEL:EtOH) and PAX7′C_6 (in CrEL:EtOH) were prepared by dissolving paclitaxel in ethanol (3 mg/ml) and adding to a solution of ethanol (final 1.5 mg/ml paclitaxel) [19]. The resulting mixture was vortexed until clear and passed through a 0.45-μm PTFE syringe filter. PAX7′C_6 was solubilized to 1.33 mg/ml in PEG-*b*-PCL. Taxol® (30 mg/ml paclitaxel in Cremophor CrEL:EtOH) and PAX7′C_6 (30 mg/ml PAX7′C_6 in CrEL:EtOH) were formulated at 1.5 mg/ml by dilution in 0.9% saline. Immediately before injection, the concentrations of paclitaxel and PAX7′C_6 were verified by reverse-phase HPLC as above.

Cell Cytotoxicity

The 6 derivatives of paclitaxel were screened for preservation of activity by incubation with each prodrug in MDA-MB-231 (Her-2/Neu negative, Estrogen receptor negative Human Breast Adenocarcinoma) and MCF-7 (Her-2/Neu negative, Estrogen receptor positive Human Breast Adenocarcinoma) cell lines. Paclitaxel and PAX7′C_6 (0.5–5,000 ng/ml) were further tested in the cancer cell lines, SK-BR-3 (Her-2/Neu positive, Estrogen receptor negative Human Breast Adenocarcinoma) and +SA (WAZ-2T; Spontaneous Mouse Breast Cancer Cell Line). PAX7′C_6 in PEG-*b*-PCL micelles was incubated with MDA-MB-231 cells (0.5–5,000 ng/ml). All cell lines were purchased from the American Type Culture Association (ATCC, Rockville, MD). MDA-MB-231 and SK-BR-3 cell lines were maintained in McCoy's 5A medium and supplemented with 10% heat-inactivated fetal bovine serum (FBS), penicillin-streptomycin solution (10 ml/l), and HEPES (6.0 g/l). MCF-7 were maintained in RMPI 1640 supplemented with 10% fetal bovine serum, 100 IU penicillin, and 100 μg/ml streptomycin, and 2 mM L-glutamine. +SA cell line was maintained in Dulbecco's Modified Eagle Medium (D-MEM) and supplemented with 10% heat-inactivated fetal bovine serum (FBS), penicillin-streptomycin solution (10 ml/l), HEPES (2.4 g/l), and sodium pyruvate (110.4 mg/l). All cell lines were incubated at 37°C in a 5% CO_2 atmosphere. MDA-MB-231, and +SA cell lines was seeded at 5,000 cells/well while SK-BR-3 cell line was seeded at 15,000 cells/well and MCF-7 were seeded at 3,000 cells/well in 96-well plates.

Alamar Blue Assay

Alamar Blue (resazurin) fluorescent dye is a facile and accurate assay to determine the cytotoxicity of many cell lines including the four cancer cell lines used in the present study [20]. The resazurin non-fluorescent compound is metabolized into the fluorescent compound resorufin by intact and viable cells. This emission of fluorescence can be quantified using a cell plate reader and the number of viable cells following treatment can be determined. Cells were counted and seeded on 96 well plates. The seeded cells were incubated at 37°C in a 5% CO_2 atmosphere for 24 h. On the day of the experiment, paclitaxel and PAX7′C_6 was dissolved in DMSO while the PAX'7C_6 formulation was dissolved in water. The formulation and each compound were diluted in medium to yield concentrations of 0.5, 1, 5, 10, 50, 100, 500, 1000, and 5000 ng/ml. Following aspiration of the medium, cells were treated with either paclitaxel, PAX7′C_6, or PAX7′C_6 PEG-*b*-PCL micelles. Additional cells were treated with either DMSO diluted in medium, water diluted in medium (for micelle comparison), or medium only as controls. Treated and control cells were incubated at 37°C in a 5% CO_2 atmosphere for 72 h. After cell plates were removed from the incubator, alamar blue (resazurin) fluorescent dye was added directly to the media (20 μl) to give a final concentration of 10% alamar blue in each well. Cell plates were incubated at 37°C in a 5% CO_2 atmosphere for an additional 3 h. Following incubation, cell plates were placed in a darkened environment for 15 min at room temperature. Next, the cell plates were placed into the Cytoflour®4000 fluorescence multi-well plate reader (Applied Biosystems, USA). Fluorescence was read at an excitation of 485 nm and an emission of 530 nm. The viable cell number (as a percent of control) in each cell line exposed to varying concentrations of paclitaxel prodrug and paclitaxel were measured. The IC_{50} values for each cell line were determined by using pharmacodynamic modeling using WinNonlin® software (Ver. 5.1).

Surgical Procedures

Male Sprague-Dawley rats (200–240 g) were obtained from Simonsen Labs (Gilroy, CA, USA) and given food (Purina Rat Chow 5001) and water ad libitum in our animal facility for at least 3 days before use. Rats were housed in temperature-controlled rooms with a 12 h light/dark cycle. The day before the pharmacokinetic experiment, the right jugular veins of the rats were catheterized with sterile silastic cannula (Dow Corning, Midland, MI, USA) under halothane

(Sigma Chemical Co. St. Louis Mo. USA) anesthesia. This involved exposure of the vessel prior to cannula insertion. After cannulation, the Intramedic PE-50 polyethylene tubing (Becton, Dickinson and Company, Franklin Lakes, NJ, USA) connected to the cannula was exteriorized through the dorsal skin. The cannula was flushed with 0.9% saline. The animals were transferred to metabolic cages and fasted overnight. Animal use protocols were approved by The Institutional Animal Care and Use Committee at Washington State University, in accordance with "Principles of laboratory animal care" (NIH publication No. 85-23, revised 1985).

Pharmacokinetic Study

Sprague-Dawley male rats with body weights ranging from 200 to 240 g were used to examine the effect of solubilizing vehicle on the pharmacokinetics of PAX7′C_6 compared to Taxol® (paclitaxel in Cremophor CrEL:EtOH) and PAX7′C_6 in CrEL:EtOH as controls. The rats were housed in a temperature-controlled room with a 12 h light/dark cycle for at least 1 week. The day before the pharmacokinetic experiment, the rats were cannulated as described above. Each of the animals was placed in separate metabolic cages, allowed to recover overnight, and fasted for 12 h before dosing. On the days of the experiment, the animals were dosed intravenously (10 mg/kg) with PAX7′C_6 formulated in PEG-*b*-PCL nanocarrier, Taxol® (paclitaxel in Cremophor CrEL:EtOH), or PAX7′C_6 (in CrEL:EtOH; $n = 10$ for each treatment group). The rats were given between 0.5 and 1 ml of each formulation as IV bolus. The utilized dose was based on previous pharmacokinetics studies that administered Taxol® and other similar delivery systems of paclitaxel [21–23]. After dosing, serial blood samples (~0.30 ml) were collected from the cannula at 0, 1 min, and 30 min, then 1, 2, 4, 6, 12, 24, and 48 h after IV administration, and the cannula flushed with 0.9% saline. After dosing and after each serial blood sampling, blinded observers were present to record any visible behavior, bleeding, or change in overall appearance of the animal as signs of acute toxicity. Each blood sample was collected into regular polypropylene microcentrifuge tubes and following centrifugation, the serum was collected and stored at −70°C until analyzed. Urine samples were also collected at 0, 2, 6, 12, 24, 48, and 72 h following IV administration and were stored at −70°C until analyzed.

Biodistribution Studies

To assess the effect of formulation on the tissue distribution of PAX7′C_6, rats ($n = 10$ for each group, 200–240 g) were cannulated and intravenously administered with Taxol® (paclitaxel in Cremophor CrEL:EtOH), PAX7′C_6 in CrEL:EtOH, or PAX7′C_6 in PEG-*b*-PCL micelles all equivalent to the previous pharmacokinetic studies. At either 6 or 24 h after formulation injection, each animal ($n = 5$ for each time point) was anaesthetized and exsanguinated by cardiac puncture. Brain, lungs, heart, liver, spleen, kidneys, urinary bladder, muscle as well as samples of whole blood and serum were collected. Tissue samples were blotted with paper towel, washed in ice-cold saline, bottled to remove excess fluid, weighed and rapidly frozen in liquid nitrogen, pulverized to a fine powder with a mortar and pestle under liquid nitrogen and stored at −70°C until assessed for drug concentrations by HPLC analysis.

Pharmacokinetic Analysis

Pharmacokinetic analysis was performed using data from individual rats for which the mean and standard error of the mean (SEM) were calculated for each group. The elimination rate constant (KE) was estimated by linear regression of the blood or plasma concentrations in the log-linear terminal phase. In order to estimate the serum concentrations (C_0) immediately after nanoformulated PAX7′C_6, PAX7′C_6 in CrEL:EtOH or Taxol® (paclitaxel in CrEL:EtOH) IV dosing, a two-compartmental model was fitted to the serum concentration versus time data using WinNonlin® software (Ver. 5.1). The estimated C_0 was then used with the actual measured serum concentrations to determine the area under the concentration-time curve (AUC). The $AUC_{0\text{-}\infty}$ was calculated using the combined log-linear trapezoidal rule for data from time of dosing to the last measured concentration, plus the quotient of the last measured concentration divided by KE. Non-compartmental pharmacokinetic methods were used to calculate mean residence time (MRT by dividing $AUMC_{0\text{-}\infty}$ by $AUC_{0\text{-}\infty}$), clearance (CL by dividing dose by $AUC_{0\text{-}\infty}$) and volume of distribution (Vd_β by dividing CL by KE). Based on the cumulative urinary excretion, the fraction excreted in urine [F_e by dividing the total cumulative amount of paclitaxel excreted in urine (ΣXu) by the dose], renal clearance (CL_r by multiplying F_e by CL), hepatic clearance ($CL_{hepatic}$ by subtracting CL_r from CL), extraction ratio [ER by dividing $CL_{hepatic}$ by hepatic flow (Q)]. The mean hepatic blood flow (Q) is approximately 3.22 l/h/kg [24]. Using the hematocrit in rat (24) of 0.48, this yields a mean hepatic plasma flow of 1.74 l/h/kg. Therefore, depending on serum or whole blood the correct hepatic flow (Q) needs to be employed.

Data Analysis

Compiled data were presented as mean and standard error of the mean (mean ± SEM). Where possible, the data were analyzed for statistical significance using NCSS Statistical and Power Analysis software (NCSS, Kaysville, UT). General Linear Model (GLM) ANOVA was employed with a value of $p < 0.05$ being considered statistically significant.

RESULTS

Solubility and Sizing

All of the paclitaxel prodrugs have greatly enhanced solubility in PEG-*b*-PCL as compared to paclitaxel. Drug-loaded micelles were readily concentrated by evaporation to achieve solubilities >5 mg/ml (Table I). Drug-loaded micelles were 27 to 44 nm in diameter as determined by DLS. Acylation increases solubility in caprolactone micelles. The decrease in the χ parameter as compared to paclitaxel demonstrates greater core-drug compatibility. The Flory-Huggins interaction parameter for these prodrug and PCL was calculated (Table I). Drugs with relatively small interac-

Table I. Solubility Parameters and Sizing of PEG-*b*-PCL Micelles Loaded with Paclitaxel Prodrugs

Prodrug	δ drug $(J/cm^3)^{1/2}$	$V_{drugcm}{}^3$/mol	Diameter (intensity), nm[c]	χ drug-PCL	log $P_{o/w}$	Prodrug: caprolactone mmol:mol[a]	Prodrug *w/w* %[a]	Solubilized mg/ml[a,b]
Paclitaxel 1	26.7	498	–	8.59	4.40 ± 0.06	<1	–	<0.2
4a	24.5	604	34 ± 4	4.55	4.43 ± 0.06	36.5	17.1	1.55 ± 0.04 (5.1 ± 0.5)
4b	23.5	700	27 ± 5	3.14	4.59 ± 0.18	31.8	16.4	1.47 ± 0.03 (2.2 ± 0.5)
4c	23.0	765	44 ± 2	2.43	4.48 ± 0.06	33.3	21.6	1.62 ± 0.03 (3.0 ± 0.9)
5a	24.5	604	32 ± 0	4.55	4.45 ± 0.03	33.4	17.8	1.42 ± 0.11
5b	23.5	700	28 ± 0	3.14	4.49 ± 0.03	34.0	17.3	1.57 ± 0.02
5c	23.0	765	37 ± 6	2.43	4.51 ± 0.04	40.0	19.8	1.85 ± 0.05

[a] Solubility and encapsulation based on 20% *w/w* prodrug loading in 0.5-mM PEG-b-PCL micelles. Results are given ± standard deviation ($n = 3$).
[b] Results in parentheses are after evaporation to 25% of original volume and refiltration (0.22-μm).
[c] Hydrodynamic diameters from DLS with Gaussian intensity weighing of drug loaded micelles prepared at 20% w/w drug; standard deviations are of the size distribution.

tion parameters, $\chi_{drug\text{-}PCL}$ <1, are well solubilized (>1:1 mmol drug: mol PCL) by PEG-*b*-PCL or PEG-*b*-PCL-*b*-PEG nanocarrier systems whereas drugs with larger interaction parameters, such as paclitaxel, are very poorly solubilized by PEG-*b*-PCL micelles. The oil-water and *n*-octanol partitioning behavior of drugs can be useful in predicting *a priori* the *in vivo* tissue distribution [25]. All of the fatty acid prodrugs had similar lipophilic, partitioning into the oil phase as compared to paclitaxel (Table I). Actually loadings are reported in Table I.

Release of PAX7′C_6 from PEG-*b*-PCL Micelles

We investigated the *in vitro* release kinetics of paclitaxel prodrug PAX7′C_6 from PEG-*b*-PCL micelles at a physiological pH of 7.4 and the nominal body temperature of 37°C. Micelles released the prodrug slowly over the course of several days (Fig. 2). Release half-lives of the PAX7′C_6 from PEG-*b*-PCL micelles was slow and without a significant burst effect. Less than 50% of PAX7′C_6 was released over a period of 2 weeks.

Cytotoxicity

Only the 7′derivative of paclitaxel with the shortest acyl-chain 7′hexonoate (PAX7′C_6) **4a**, maintained activity similar to unmodified paclitaxel **1** in MDA-MB-231 and MCF-7 cells. The 2′derivatives (**5a**, **5b**, **5c**), 7′dodeconoate (**4b**) and 7′palmitate (**4c**) were not active, i.e. IC_{50} >1 μM (Table II). For this reason, further studies were pursued using only the PAX7′C_6 prodrug.

The paclitaxel prodrug, PAX7′C_6, showed activity in the nanomolar range with IC_{50}'s similar to paclitaxel in all breast cancer cells tested (Table II). In Fig. 3, we report the activity in MDA-MB-231 cells as a representative graph. In both SK-BR-3 and MDA-MB-231, PAX7′C_6, showed similar activity with no statistically significant differences (IC_{50} = 91.7 nM and 288 nM, respectively) to paclitaxel (IC_{50} = 213 and 326 nM). PAX7′C_6 was also found active in +SA (WAZ-2) murine breast cancer cells with an IC_{50} of 129 nM which was comparable to paclitaxel at an IC_{50} of 93.9 nM. Solubilization of PAX7′C_6 in PEG-PCL micelles did not alter activity *in vitro* in MDA-MB-231 cells (IC_{50} = 114 nM; Fig. 3).

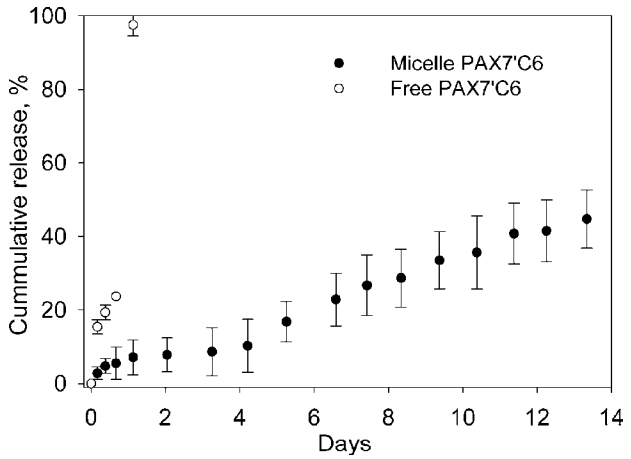

Fig. 2. *In vitro* release of PAX7′C_6 prodrug from 0.5-mM PEG-*b*-PCL micelles in ddH_2O at 37°C and pH 7.4. (mean ± SD, $n = 4$) Micelles were prepared with 20% *w/w*; actual incorporations are reported in Table I. An equal quantity of prodrug dissolved in 100 μl of ethanol and injected into a separate cassette was a control.

Table II. Prodrug cytotoxicity against SK-BR-3, MDA-MB-231, MCF-7, and +SA Breast Cancer Cell Lines. Cells Were Incubated 72 Hours with each Prodrug and Cell Viability was Assessed Through Alamar Blue Assay ($n = 4$)

	IC_{50} (nM ± SD)			
	SK-BR-3	MDA-MB-231	MCF-7	+ SA
Paclitaxel 1	213 ± 92	326 ± 128[a]	47.0 ± 18.1	93.9 ± 42.9
PAX7′C6 4a	91.7 ± 37.5	288 ± 94	60.1 ± 26.2	129 ± 28
4b	>1 μM	>1 μM	>1 μM	>1 μM
4c	>1 μM	>1 μM	>1 μM	>1 μM
5a	>1 μM	>1 μM	>1 μM	>1 μM
5b	>1 μM	>1 μM	>1 μM	>1 μM
5c	>1 μM	>1 μM	>1 μM	>1 μM
PAX7′C6 in micelles	–	114 ± 30[a]	–	–

[a] Denotes statistical significant difference ($P < 0.05$) between paclitaxel and PAX7′C6, or paclitaxel and PAX7′C6 in micelles.

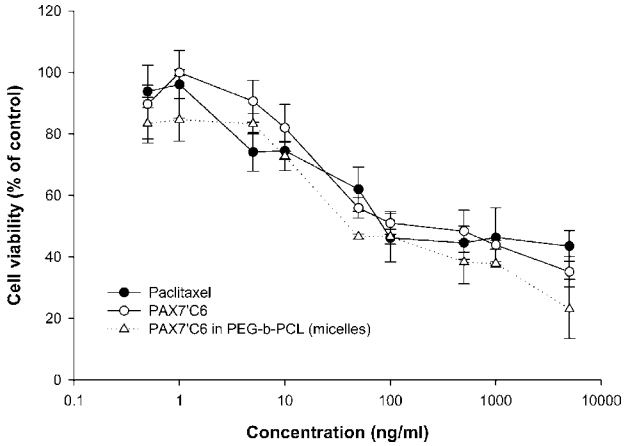

Fig. 3. Anti-Cancer Activity of Control and PAX7′C_6 formulations in A) SK-BR-3 cells, B) MDA-MB-231 cells, and C) +SA cells (mean ± SEM, $n = 4$).

Pharmacokinetics of Polymeric Micellar PAX-7C_6 After Intravenous Administration

The serum paclitaxel and PAX7′C_6 concentration vs time profiles observed for the three formulations were not parallel (Fig. 4). It was observed that Taxol® (paclitaxel in CrEL:EtOH) was rapidly cleared from the body allowing its detection up to 6 h. The paclitaxel concentrations after the prodrug PAX7′C_6 was dissolved in CrEL:EtOH demonstrated rapid clearance and no detection of paclitaxel 6 h post-dosing. However, when PAX7′C_6 was loaded in PEG-*b*-PCL micelles a sustained release and conversion of paclitaxel was observed up to 24 h having higher concentrations than the paclitaxel concentrations in the Taxol® and PAX7′C_6 in CrEL:EtOH controls (Fig. 4). This indicates that the micellar system provides an improved delivery and a more sustained release. Also, the concentrations of PAX7′C_6 prodrug were detected in serum, and the concentrations in CrEL:EtOH were significantly lower compared to the PEG-*b*-PCL formulation. Furthermore, the concentrations of prodrug (PAX7′C_6) after dissolution in CrEL:EtOH were detected up to 12 h, while PAX7′C_6 after loading in PEG-*b*-PCL micelles was detected in serum up to 48 h. There were significant differences in serum elimination phase $t_{1/2}$ of paclitaxel: the serum half-life of paclitaxel from PAX7′C_6 in PEG-*b*-PCL (5.602 ± 1.656 h) being significantly higher than both Taxol® and paclitaxel from PAX7′C_6 in CrEL:EtOH (1.548 ± 0.122 h and 1.333 ± 0.055 h, respectively). Higher elimination phase $t_{1/2}$ of the prodrug (PAX7′C_6) was also observed after loading in PEG-*b*-PCL (6.946 ± 0.479 h) compared to the prodrug dissolved in CrEL:EtOH (5.131 ± 0.989 h; Table III).

Pharmacokinetic parameters of paclitaxel and PAX7′C_6 in PEG-PCL compared to Taxol® and PAX7′C_6 in CrEL:EtOH control formulations are presented (Table III). The micelle carrier increased the AUC values in serum of paclitaxel and PAX7′C_6 by 7-fold and 24-fold when compared to Taxol® and PAX7′C_6 in CrEL:EtOH, respectively. A decrease in total clearance (CL_{tot}) of 8-fold and 25-fold was also observed for paclitaxel and PAX7′C_6 from PAX7′C_6 in PEG-PCL compared to Taxol® and PAX7′C_6 from PAX7′C_6 in CrEL:EtOH, respectively. The total clearance (CL_{tot}) value of paclitaxel from PAX7′C_6 in CrEL:EtOH (6.909 ± 1.070 l/h/kg) suggests a very rapidly clearance from the serum. The volume of distribution at the elimination phase (Vd_β) in serum was found to decrease by 2-fold and 18-fold for the micelle nanocarrier compared to Taxol® and PAX7′C_6 in CrEL:EtOH, respectively. These observed differences in clearance, AUC, volume of distribution, and half-life can be summarized by the differences in the reported mean residence time (MRT). The micelle formulation increased the MRT of paclitaxel by fourfold, while the micellar system decreased the MRT of the PAX7′C_6 prodrug in serum by 1.8-fold (Table III).

The mean hepatic blood flow (Q) is approximately 3.22 l/h/kg [24]. Using a hematocrit value in rat [24] of 0.48, yields a mean hepatic plasma flow of 1.74 l/h/kg. While the CL_{tot} value for paclitaxel from Taxol® is 1.556 ± 0.400 l/h/kg, the micellar system reduces the total clearance of paclitaxel by eightfold to 0.196 ± 0.005 l/h/kg. A reduction in the total clearance of 26-fold was also observed for the prodrug PAX7′C_6 in PEG-*b*-PCL compared to the prodrug dissolved in CrEL:EtOH (Table III). Therefore, the nanocarrier induces a longer systemic residence due to a more pronounced sustained release *in vivo* that allows for the drugs to reside longer in the body (higher MRT values).

The terminal urine half-life of paclitaxel significantly increased after micellar formulation: the PEG-*b*-PCL formulation increased the half-life (15.827 ± 0.808 h) by 1.4-fold compared to both paclitaxel from Taxol® (10.932 ± 2.091 h) and paclitaxel from PAX7′C_6 in CrEL:EtOH (10.898 ± 1.526 h). An increase of 2.4-fold in the urine half-life for the prodrug PAX7′C_6 in PEG-*b*-PCL (17.102 ± 1.907 h) was observed compared to the urine half-life of PAX7′C_6 from PAX7′C_6 in CrEL:EtOH (7.042 ± 0.290 h; Table III). Three plots are commonly employed to represent urinary excretion. The total amount excreted in urine plot is often used to determine the amount of drug excreted in urine through the length of sampling.

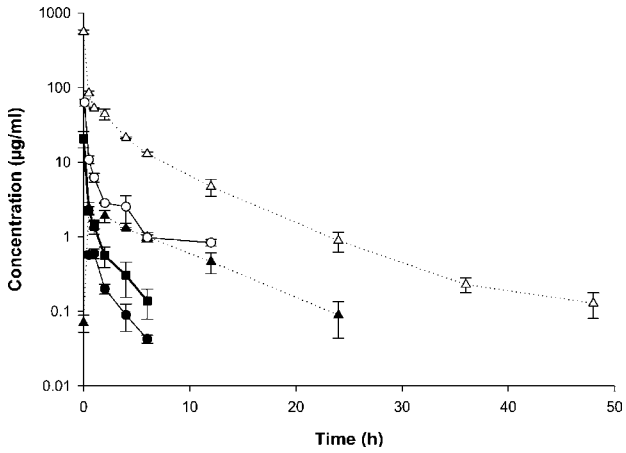

Fig. 4. Concentration-time profile in serum of paclitaxel after iv administration of control Taxol® (paclitaxel in Cremophor EL:Ethanol: *filled squares*); paclitaxel (*filled circles*) and PAX7′C_6 (*open circles*) after iv administration of control PAX7′C_6 in Cremophor EL:Ethanol: and paclitaxel (*filled triangles*) and PAX7′C_6 (*open triangles*) after iv administration of PAX7′C_6 in PEG-*b*-PCL. The intravenous dose for all the formulations was 10 mg/kg to rats (mean ± SEM, $n = 10$ per group).

Table III. Pharmacokinetics of Paclitaxel After iv Administration of Control Taxol® (Paclitaxel in Cremophor EL:Ethanol); Paclitaxel and PAX7′C_6 After iv Administration of Control PAX7′C_6 in Cremophor EL:Ethanol; and Paclitaxel and PAX7′C_6 after iv Administration of PAX7′C_6 in PEG-*b*-PCL. The Intravenous Dose for all the Formulations was 10 mg/kg to Rats (mean ± SEM, $n = 10$ per group)

Pharmacokinetic Parameter	Paclitaxel from Taxol® Control	Paclitaxel from PAX7′C_6 in CrEL:EtOH	Paclitaxel from PAX7′C_6 in PEG-*b*-PCL	PAX7′C_6 from PAX7′C_6 in CrEL:EtOH	PAX7′C_6 from PAX7′C_6 in PEG-*b*-PCL
AUC_{inf} (μgh/ml)	7.194 ± 1.495	1.519 ± 0.235[a]	51.113 ± 1.362[b,c]	16.247 ± 3.062	392.758 ± 31.501[d]
Vd_{β} (L/kg)	3.377 ± 0.687	13.125 ± 1.498[a]	1.602 ± 0.504[b,c]	4.678 ± 0.765	0.259 ± 0.030[d]
CL_{renal} (L/h/kg)	0.900 ± 0.203	0.635 ± 0.072	0.014 ± 0.002[b,c]	0.004 ± 0.001	$3.378 \times 10^{-06} \pm 4.291 \times 10^{-07}$[d]
$CL_{hepatic}$ (L/h/kg)	0.655 ± 0.220	6.274 ± 1.094[a]	0.182 ± 0.004[b,c]	0.656 ± 0.121	0.026 ± 0.002[d]
CL_{tot} (L/h/kg)	1.556 ± 0.400	6.909 ± 1.070[a]	0.196 ± 0.005[b,c]	0.661 ± 0.122	0.026 ± 0.002[d]
F_e (%)	58.913 ± 5.953	9.695 ± 1.805[a]	6.959 ± 0.851[b]	0.656 ± 0.081	0.014 ± 0.003[d]
KE (h^{-1})	0.453 ± 0.033	0.522 ± 0.022	0.145 ± 0.036[b,c]	0.145 ± 0.027	0.101 ± 0.007
$t_{1/2}$ (h) serum	1.548 ± 0.122	1.333 ± 0.055	5.602 ± 1.656[b,c]	5.131 ± 0.989	6.946 ± 0.479
$t_{1/2}$ (h) urine	10.932 ± 2.091	10.898 ± 1.526	15.827 ± 0.808[b,c]	7.042 ± 0.290	17.102 ± 1.947[d]
MRT (h)	1.100 ± 0.214	1.912 ± 0.103[a]	4.291 ± 0.767[b,c]	7.635 ± 1.107	4.138 ± 0.380[d]
Extraction ratio (ER)	0.377 ± 0.126	3.606 ± 0.628[a]	0.105 ± 0.002[b,c]	0.377 ± 0.070	0.015 ± 0.001[d]

[a] Denotes statistical significant difference ($P < 0.05$) between paclitaxel after iv administration of control Taxol® (paclitaxel in Cremophor EL:Ethanol) and paclitaxel after iv administration of control PAX7′C_6 in Cremophor EL:Ethanol.
[b] Denotes statistical significant difference ($P < 0.05$) between paclitaxel after iv administration of control Taxol® (paclitaxel in Cremophor EL:Ethanol) and paclitaxel after iv administration of PAX7′C_6 in PEG-*b*-PCL.
[c] Denotes statistical significant difference ($P < 0.05$) between paclitaxel after iv administration of control PAX7′C_6 in Cremophor EL:Ethanol and paclitaxel after iv administration of PAX7′C_6 in PEG-*b*-PCL.
[d] Denotes statistical significant difference ($P < 0.05$) between PAX7′C_6 after iv administration of control PAX7′C_6 in Cremophor EL:Ethanol and PAX7′C_6 after iv administration of PAX7′C_6 in PEG-*b*-PCL.

The amount remaining to be excreted (ARE) plot is often used to drug excretion in urine over time. In addition, the rate of urinary excretion plot describes elimination rate into urine.

The total amount excreted in urine plot (Fig. 5a) exhibits that paclitaxel from Taxol® is excreted in higher amounts compared to the other formulations and by 24 h post-dose the majority of paclitaxel is excreted. The fraction excreted unchanged (Fe) of paclitaxel from Taxol® (58.913 ± 5.923%) was reduced by sixfold and eightfold compared to paclitaxel from PAX7′C_6 in CrEL:EtOH (9.695 ± 1.805%) and paclitaxel from PAX7′C_6 in PEG-*b*-PCL (6.959 ± 0.851%; Table III). This indicates a change in the clearance pattern of paclitaxel from the prodrug and after loading in the micellar system. Furthermore, it can be observed that higher amounts of paclitaxel are released from PAX7′C_6 in PEG-*b*-PCL compared to the amount of paclitaxel released from the prodrug in CrEL:EtOH. The amount of paclitaxel from PAX7′C_6 in PEG-*b*-PCL excreted in urine is relatively constant even 72 h post-dosing compared to the amount of paclitaxel released from PAX7′C_6 in CrEL:EtOH that is mostly excreted 24 h post-dosing (Fig. 5a) suggesting the micellar formulation provides a sustained conversion of the prodrug to paclitaxel. The amounts of prodrug (PAX7′C_6) excreted as such in urine are significantly lower than the amounts of paclitaxel excreted in urine. The amount of PAX7′C_6 from PAX7′C_6 in CrEL:EtOH represent only 15.80% of the total amount of paclitaxel excreted in urine. While the amount of PAX7′C_6 from PAX7′C_6 in PEG-*b*-PCL represent only 0.05% of the total amount of paclitaxel excreted in urine from the same micellar formulation. Also, the micellar system reduces the Fe value (0.014 ± 0.003%) by 48-fold compared to the Fe value of the prodrug from PAX7′C_6 in PEG-*b*-PCL (0.656 ± 0.081%; Table III).

The amount remaining to be excreted (ARE) plot (Fig. 5b) indicates that paclitaxel from Taxol® follows a rapid initial excretion in urine and 24 h post-dosing most of the paclitaxel is excreted. A similar excretion pattern was observed for paclitaxel from PAX7′C_6 in CrEL:EtOH, while paclitaxel from PAX7′C_6 in PEG-*b*-PCL has a steady initial excretion in urine followed by a rapid decline in excretion indicating that at 72 h post-dosing there remains paclitaxel still to be excreted from the micellar system with a consequent longer half-life. These observations correlate with the reported urine terminal half-lives: paclitaxel from Taxol® which has a similar urine terminal half-life (10.932 ± 2.091 h) compared to paclitaxel from CrEL:EtOH (10.898 ± 1.526 h), while the micellar system increases the half-life of paclitaxel by 1.4-fold to 15.827 ± 0.808 h (Table III). The ARE plot also indicates that the prodrug (PAX7′C_6) from PAX7′C_6 in CrEL:EtOH is mainly excreted in urine 12 h post-dosing, while the ARE plot of the prodrug from PAX7′C_6 in PEG-*b*-PCL exhibits that the prodrug has a more constant steady excretion of the prodrug (Fig. 5b). These differences can be observed in more detail by the significant differences in half-lives in urine, in which micellar system increases the urine $t_{1/2}$ by 2.5-fold (17.102 ± 1.947 h) compared to the prodrug formulation in CrEL:EtOH (7.042 ± 0.290 h; Table III). The rate plots (Fig. 5c) demonstrate that independent of the formulation system paclitaxel and the prodrug (PAX7′C_6) are excreted at the same rate.

Furthermore, as mentioned above it was determined that paclitaxel from Taxol® is mainly cleared by renal clearance (Fe value equal to 58.913 ± 5.923%) and that the prodrug and micellar system change the clearance route to a predominantly non-renal mechanism (Fe values of 9.695 ± 1.805% for paclitaxel from PAX7′C_6 in CrEL:EtOH and 6.959 ± 0.851% for paclitaxel from PAX7′C_6 in PEG-*b*-PCL). Therefore, the

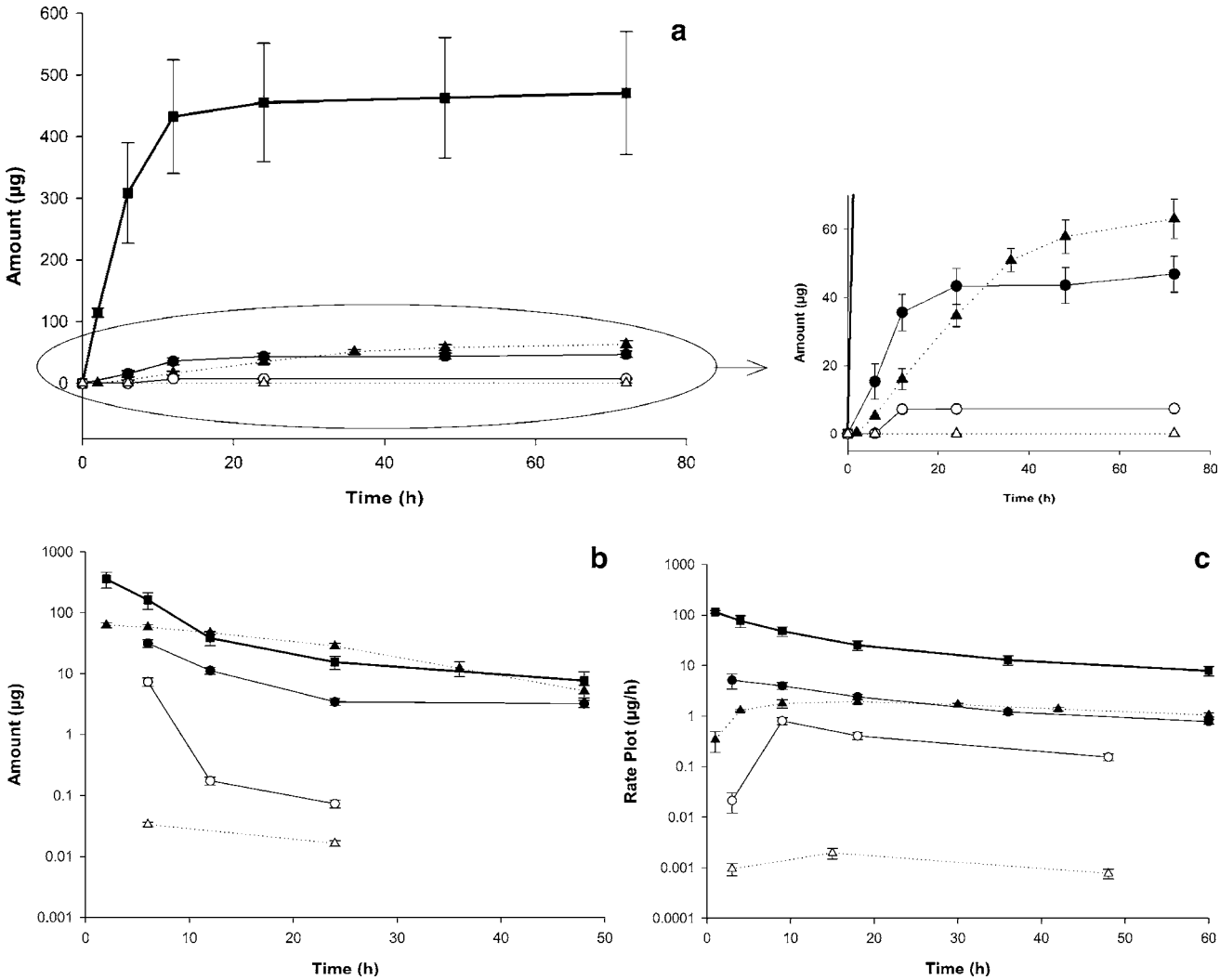

Fig. 5. **a** Total amount excreted in urine plot, **b** amount remaining to be excreted in urine (ARE) plot, and **c** urinary rate plot of paclitaxel after iv administration of control Taxol® (paclitaxel in Cremophor EL:Ethanol; *filled squares*); paclitaxel (*filled circles*) and PAX7′C_6 (*open circles*) after iv administration of control PAX7′C_6 in Cremophor EL:Ethanol; and paclitaxel (*filled triangles*) and PAX7′C_6 (*open triangles*) after iv administration of PAX7′C_6 in PEG-*b*-PCL. The intravenous dose for all the formulations was 10 mg/kg to rats (mean ± SEM, $n = 10$ per group).

micellar system invokes a significant change in the pattern of clearance from a predominantly renal clearance to a clearance predominantly via non-renal routes.

Observations performed by blinded observers reported that almost immediately between 12 h post-IV dosing of Taxol® control formulation and PAX7′C_6 in CrEL:EtOH the rats presented nose bleeding, disorientation, heavy breathing, slight decrease in response to sound, and 30% of the Taxol® control subjects died within 48–72 h post-dose. The animals that received the PAX7′C_6 in PEG-*b*-PCL formulation did not display adverse effects for the first 24 h, but demonstrated mild diarrhea and nose bleeding after 48 h post-dose, nonetheless, 100% of the animals survived until the end of the experiment (72 h post-dose).

Biodistribution

Quantifiable amounts of paclitaxel (except in brain in some instances) and PAX7′C_6 were observed in all assayed tissues. The tissue collection was performed at 6 h and 24 h post IV administration at 10 mg/kg. The order in concentrations from highest to lowest for the paclitaxel from control Taxol® (paclitaxel in CrEL:EtOH) 6 h post dose was spleen>liver>lung>muscle>heart>urinary bladder>kidney>blood>serum and paclitaxel was not effectively measured in brain (below detectable levels 0.02 µg/ml). The micellar system provided changes in the tissue distribution of paclitaxel and the prodrug PAX7′C_6 6 h post dose. The order in concentrations from highest to lowest for the paclitaxel from PAX7′C_6 in PEG-*b*-PCL was liver>brain>kidney>lung>serum>blood>muscle>urinary bladder>heart>spleen. It was also observed that all the tissues presented lower paclitaxel concentrations compared to paclitaxel concentrations from Taxol® control, but the paclitaxel serum concentrations were significantly higher than the control formulation. The order of tissue concentrations from highest to lowest for the PAX7′C_6 from PAX7′C_6 in PEG-*b*-PCL was lung>liver>kidney>blood>spleen>urinary bladder>heart>serum>muscle>brain. In this instance it was observed that the concentration of prodrug in serum and in all the tissues was significantly higher

Table IV. Mean Concentrations (μg/g of Tissue) of Paclitaxel and PAX7′C_6 in Rat Tissues (and Tissue to Serum Ratios—Kp Values—in Parenthesis) Measured at 6 h post iv Administrations of Control Taxol® (Paclitaxel in Cremophor EL/Ethanol) and PAX7′C_6 in PEG-*b*-PCL in Plasma after iv Administration (10 mg/kg; mean ± SEM, $n = 4$)

Tissue	Paclitaxel from Taxol® Control	Paclitaxel from PAX7′C_6 in PEG-*b*-PCL	PAX7′C_6 from PAX7′C_6 in PEG-*b*-PCL
Serum	0.066 ± 0.003	0.464 ± 0.095[a]	10.062 ± 0.913[b,c]
Whole Blood	1.463 ± 0.097 (22.110 ± 1.473)	0.332 ± 0.139[a] (0.716 ± 0.300)[a]	14.730 ± 5.954[b,c] (1.464 ± 0.592)[b]
Liver	17.042 ± 5.559 (257.498 ± 83.988)	1.171 ± 0.184[a] (2.526 ± 0.396)[a]	23.053 ± 7.598 (2.291 ± 0.755)[b]
Kidney	3.989 ± 1.221 (60.272 ± 18.449)	0.669 ± 0.147[a] (1.445 ± 0.317)[a]	19.129 ± 4.109[b,c] (1.901 ± 0.408)[b]
Spleen	33.419 ± 0.543 (504.942 ± 8.198)	0.274 ± 0.078[a] (0.592 ± 0.168)[a]	14.397 ± 2.556[b,c] (1.431 ± 0.254)[b,c]
Brain	<0.02 (<0.30)	0.736 ± 0.181[a] (1.587 ± 0.390)[a]	0.707 ± 0.191[b] (0.070 ± 0.019)[b,c]
Muscle	12.056 ± 3.054 (182.155 ± 46.139)	0.323 ± 0.025[a] (0.696 ± 0.054)[a]	9.884 ± 1.589[c] (0.982 ± 0.158)[b,c]
Lung	16.425 ± 5.098 (248.170 ± 77.028)	0.606 ± 0.126[a] (1.307 ± 0.271)[a]	33.399 ± 9.000[b,c] (3.319 ± 0.894)[b,c]
Heart	11.066 ± 2.561 (167.200 ± 38.698)	0.294 ± 0.065[a] (0.635 ± 0.140)[a]	12.086 ± 2.503[c] (1.201 ± 0.249)[b,c]
Urinary bladder	7.651 ± 0.577 (115.603 ± 8.712)	0.313 ± 0.072[a] (0.674 ± 0.155)[a]	12.643 ± 2.682[b,c] (1.256 ± 0.267)[b,c]

[a] Denotes statistical significant difference ($P < 0.05$) between paclitaxel after iv administration of control Taxol® (paclitaxel in Cremophor EL:Ethanol) and paclitaxel after iv administration of PAX7′C_6 in PEG-*b*-PCL.
[b] Denotes statistical significant difference ($P < 0.05$) between paclitaxel after iv administration of control Taxol® (paclitaxel in Cremophor EL:Ethanol) and PAX7′C_6 after iv administration of PAX7′C_6 in PEG-*b*-PCL.
[c] Denotes statistical significant difference ($P < 0.05$) between paclitaxel after iv administration of PAX7′C_6 in PEG-*b*-PCL and PAX7′C_6 after iv administration of PAX7′C_6 in PEG-*b*-PCL.

than the concentration of paclitaxel from the control formulation and from the micellar formulation (except in liver which was not significantly different than the concentrations from the control formulation; Table IV).

The tissue distribution changed 24 h post dose demonstrating that the order in concentrations from highest to lowest for the paclitaxel from Taxol® control was lung>spleen>heart>kidney>urinary bladder>liver>muscle>brain>blood>serum. The micellar system provided changes in the tissue distribution of paclitaxel and the prodrug PAX7′C_6 24 h post dose. The order in concentrations from highest to lowest for the paclitaxel from PAX7′C_6 in PEG-*b*-PCL was urinary bladder>lung>heart>liver>spleen>kidney>muscle>blood> serum, and paclitaxel was also not effectively measured in brain (below detectable levels 0.02 μg/ml). It was also observed that all the tissues and serum presented lower paclitaxel concentrations compared to paclitaxel concentrations from Taxol® control. The order of concentrations from highest to lowest for the PAX7′C_6 from PAX7′C_6 in PEG-*b*-PCL was very similar to the one exhibited by paclitaxel from Taxol® control and it was lung>spleen>urinary bladder>kidney> heart>liver>muscle>brain>blood>serum. In this instance, it was observed that the concentrations of prodrug in serum were significantly higher than the concentrations of paclitaxel from both the control formulation and from the micellar formulation. Furthermore, it was observed that the concentrations of prodrug in all the tissues were significantly lower than the concentrations of paclitaxel from both the control formulation and from the micellar formulation (except in brain, muscle, and urinary bladder; Table V).

The tissue to serum ratio (Kp) values for all the tissues after iv administration of Taxol® control ranged from 20–500 6 h post dose, while significant lower Kp values were observed for paclitaxel (0.5–2.5) and PAX7′C_6 (0.07–3.3) after administration of PAX7′C_6 in PEG–b–PCL (Fig. 6a).

Table V. Mean Concentrations (μg/g of Tissue) of Paclitaxel and PAX7′C_6 in Rat Tissues (and Tissue to Serum Ratios—Kp Values—in Parenthesis) Measured at 24 h Post iv Administrations of Control Taxol® (Paclitaxel in Cremophor EL:Ethanol) and PAX7′C_6 in PEG-*b*-PCL in Plasma after iv Administration (10 mg/kg; mean ± SEM, $n = 4$)

Tissue	Paclitaxel from Taxol® Control	Paclitaxel from PAX7′C_6 in PEG-*b*-PCL	PAX7′C_6 from PAX7′C_6 in PEG-*b*-PCL
Serum	0.036 ± 0.001	0.021 ± 0.002[a]	0.163 ± 0.012[b,c]
Whole Blood	0.039 ± 0.001 (1.104 ± 0.065)	0.074 ± 0.002[a] (2.984 ± 0.088)[a]	0.173 ± 0.032[b,c] (1.042 ± 0.113)[c]
Liver	4.801 ± 0.828 (132.581 ± 13.956)	1.049 ± 0.222[a] (49.018 ± 2.024)[a]	3.140 ± 0.333[b,c] (17.986 ± 0.803)[b,c]
Kidney	9.243 ± 1.593 (264.888 ± 36.473)	1.009 ± 0.002[a] (48.941 ± 8.316)[a]	4.474 ± 0.361[b,c] (28.164 ± 5.921)[b,c]
Spleen	20.784 ± 6.064 (593.083 ± 153.607)	1.034 ± 0.208[a] (44.401 ± 5.513)[a]	7.075 ± 0.541[b,c] (44.515 ± 9.180)[b]
Brain	0.239 ± 0.029 (6.950 ± 1.091)	<0.02[a] (<0.96)[a]	1.319 ± 0.021[b,c] (7.595 ± 0.347)[c]
Muscle	1.482 ± 0.396 (42.159 ± 13.910)	0.653 ± 0.045[a] (31.283 ± 3.234)	2.136 ± 0.022[b,c] (13.288 ± 1.613)[b,c]
Lung	59.914 ± 10.542 (1716.809 ± 242.728)	1.690 ± 0.114[a] (82.918 ± 19.619)[a]	12.713 ± 1.240[b,c] (80.212 ± 18.158)[b]
Heart	13.094 ± 2.659 (354.878 ± 83.265)	1.056 ± 0.161[a] (49.869 ± 0.966)[a]	3.875 ± 1.288[b,c] (23.084 ± 4.842)[b,c]
Urinary bladder	5.841 ± 0.430 (164.041 ± 23.201)	3.602 ± 0.395[a] (189.009 ± 38.093)	6.231 ± 0.321[c] (38.553 ± 3.115)[b,c]

[a] Denotes statistical significant difference ($P < 0.05$) between paclitaxel after iv administration of control Taxol® (paclitaxel in Cremophor EL:Ethanol) and paclitaxel after iv administration of PAX7′C_6 in PEG-*b*-PCL.
[b] Denotes statistical significant difference ($P < 0.05$) between paclitaxel after iv administration of control Taxol® (paclitaxel in Cremophor EL:Ethanol) and PAX7′C_6 after iv administration of PAX7′C_6 in PEG-*b*-PCL.
[c] Denotes statistical significant difference ($P < 0.05$) between paclitaxel after iv administration of PAX7′C_6 in PEG-*b*-PCL and PAX7′C_6 after iv administration of PAX7′C_6 in PEG-*b*-PCL.

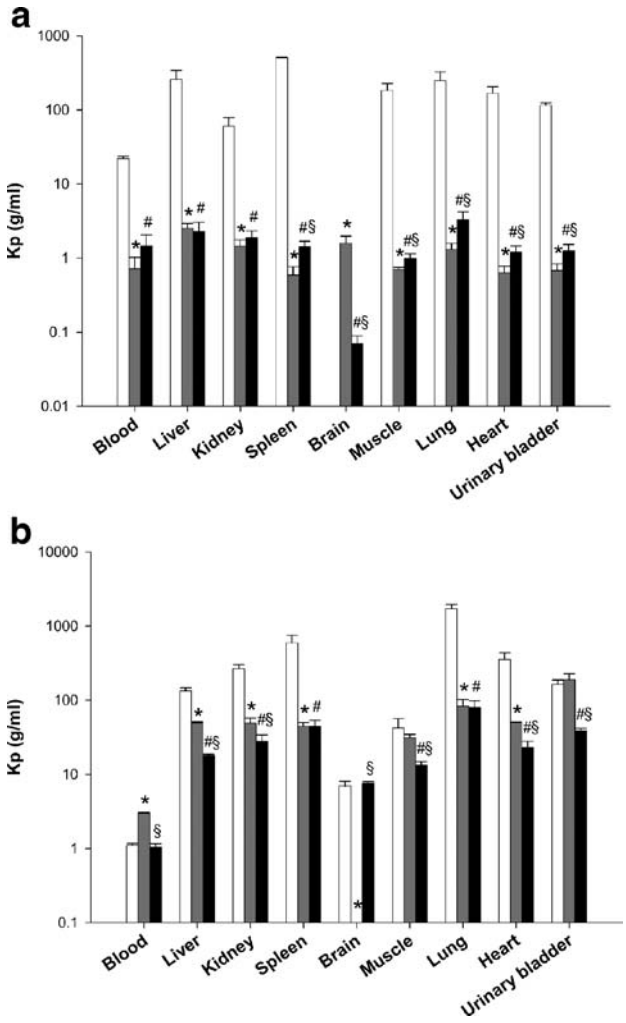

Fig. 6. Tissue to serum ratios (K_p) measured at **a** 6h and **b** 24 h post-iv administration of paclitaxel (*open squares*) from control Taxol® (paclitaxel in Cremophor EL:Ethanol), and paclitaxel (*grey squares*) and PAX7′C_6 (*filled squares*) after iv administration of PAX7′C_6 in PEG-*b*-PCL (10 mg/kg) to rats (mean ± SEM, $n = 10$ per group). *Asterisk* denotes statistical significant difference ($P < 0.05$) between paclitaxel from control Taxol® (paclitaxel in Cremophor EL:Ethanol) and paclitaxel from PAX7′C_6 in PEG-*b*-PCL. *Number sign* denotes statistical significant difference ($P < 0.05$) between paclitaxel from control Taxol® (paclitaxel in Cremophor EL:Ethanol) and PAX7′C_6 from PAX7′C_6 in PEG-*b*-PCL. *Section sign* denotes statistical significant difference ($P < 0.05$) between paclitaxel from PAX7′C_6 in PEG-*b*-PCL and PAX7′C_6 from PAX7′C_6 in PEG-*b*-PCL.

These differences in Kp values might be attributed to the differences in disposition and clearance of paclitaxel and the prodrug between the control and the micellar formulations. This can be observed based on the significantly higher concentrations in serum of paclitaxel (0.464 ± 0.095 μg/ml) and PAX7′C_6 (10.062 ± 0.913 μg/ml) after administration of the micellar prodrug formulation compared to the paclitaxel serum concentration (0.066 ± 0.003 μg/ml) after administration of control Taxol® formulation (Table IV). Furthermore, 24 h post dose the Kp values for all the tissues after Taxol® control ranged from 1–1,700, while significantly lower Kp values were observed for paclitaxel (3–190) and PAX7′C_6 (1-80) after PAX7′C_6 in PEG-*b*-PCL, except for the Kp in blood (Fig. 6b). However, it can be noted at this time point that the serum concentration of paclitaxel after iv administration of control Taxol® (0.036 ± 0.001 μg/ml) was significantly higher than the serum concentration of paclitaxel (0.021 ± 0.002 μg/ml) after administration of the micellar formulation and significantly lower than the PAX7′C_6 in PEG-*b*-PCL (0.163 ± 0.012 μg/ml; Table V).

It was also observed that the concentrations of PAX7′C_6 after administration of PAX7′C_6 in PEG-*b*-PCL in the different tissues 6 h and 24 h post dose are similar to the concentrations of paclitaxel after control Taxol®. However, at both time points also significant concentrations of paclitaxel were quantified indicating the conversion of PAX7′C_6 to paclitaxel occurred. Furthermore, the significant amounts of PAX7′C_6 found in all the tissues indicate that the prodrug is still available for posterior conversion to paclitaxel that would lead to higher residence time and availability to exert its pharmacological activity.

DISCUSSION

Cremophor® EL (polyoxyethylated castor oil) has been related to various side effects such as hypersensitivity reactions, nephrototoxicity, and neuroreactions after intravenous administrations of Taxol® [26]. In order to prevent these reactions, patients need to be premedicated with corticosteroids and antihistamines, and Taxol® has to be administered via a 1–24 h infusion [27,28]. This has led to the development of different modified formulations of paclitaxel that do not contain Cremophor® EL [29–31]. Thus, the objective of this study was to develop novel delivery systems that can act as an effective alternative to DMA, PEG, and Tween 80, Cremophor, or ethanol for paclitaxel solubilization. Further objectives included modifying the rate of release and disposition of paclitaxel, to increase paclitaxel's plasma residence, to ultimately make paclitaxel safer for human administration, and to reduce toxicity-related effects by providing a more effective carrier that can allow for the use of lower doses.

There is precedence of the use of lipophilic prodrugs in oil-based delivery systems that have shown improved solubility [16]. For instance, solubilization of a lipophilic paclitaxel oleate prodrug in a cholesterol nanoemulsion resulted in improved efficacy but high liver uptake of the prodrug [32]. The PEG-*b*-PCL micelle formulations demonstrated significant differences in pharmacokinetic parameters from the Taxol® control and PAX7′C_6 in CrEL:EtOH control formulation (Table III). The significant changes in AUC indicate a higher degree of *in vivo* stability of the PEG-PCL micelle formulations constituting a long circulating delivery system that facilitates accumulation of drug in tumors by enhanced permeation and retention (EPR) effect [7]. In addition to the EPR effect, it has been observed that nanoparticles <50 nm in diameter rapidly accumulate in vasculated tumors [33] allowing highly localized and improved delivery of paclitaxel.

The solubilization of PAX7′C_6 in PEG-*b*-PCL micelles led to a change in biological fate characterized by an increase in AUC and a reduction in CL_{tot} and (Vd_β) for the solubilized drug. The micellar system increased the volume of distribution (Vd_β) indicating that the prodrug and paclitaxel

are extensively distributed. These results suggest a large role played by the carrier system in influencing the distribution of drugs *in vivo* and how the body handles micellar systems based on their physicochemical properties. Similar increases in volumes of distribution have been previously reported for other carrier-entrapped paclitaxel formulations [21,22,34]. These changes in disposition correlate with the results of the pharmacokinetics studies by Dhanikula *et al.* [21] who recently reported similar trends in pharmacokinetics and tissue distribution in mice after administration of covalently linked paclitaxel to poloxamer 407, and by Aliabadi *et al.* [11], who recently reported altered disposition in cyclosporine loaded PEG-*b*-PCL micelles in rats. Therefore, the encapsulation of the PAX7′C_6 paclitaxel prodrug in PEG-PCL micelles caused a significant increase in residence time in the serum, longer half-life in urine, and provided a more sustained release *in vivo*, allowing longer residence and circulation in the body.

Different studies have assessed tissue distribution of Taxol® [35,36] indicating that after intravenous administration it mainly distributes to kidney, lung, heart, and spleen similar to our results indicating uptake by the monomolecular phagocyte system. Furthermore, paclitaxel physically entrapped with poly(D,L-lactide)-*b*-methoxy PEG micelles exhibited higher concentration in the lung followed by kidney, liver, heart and spleen [34], while paclitaxel conjugated to poly(glutamic acid) reported higher affinity for the liver followed by spleen and kidney [35] compared to Taxol®. Both of these studies using carrier mediated delivery systems compare and parallel our findings. In our study it was observed that conversion of PAX7′C_6 prodrug into paclitaxel occurred in the serum and that there was a significant reduction in the distribution to the heart, which may have clinical significance since paclitaxel therapy has been related with cardiotoxicity in combination therapies [37]. In *in vitro* experiments, both PAX7′C_6 alone and in formulation showed activity similar to paclitaxel. Examination of PAX7′C_6 pharmacodynamics in rodent xenografts of human breast tumor cells is currently ongoing. Overall, this study indicates that this nanocarrier system coupled with PAX-7′C_6 has potential for further pre-clinical and clinical cancer studies.

CONCLUSIONS

The PEG-*b*-PCL polymeric micelle system allowed for the uptake, protection, and retention of the water insoluble prodrug PAX-7′C_6 by increasing the half-life, the mean residence time, and the area under the curve, at the same time reducing the volume of distribution, while stabilizing the micellar structure in a biological environment. Based on our results it seems that the PEG-*b*-PCL micelles might be of the appropriate size and core/shell properties to escape the uptake by the reticuloendothelial system and stay stable during plasma circulation for longer periods more effectively.

ACKNOWLEDGMENT

This research was supported by NIH grant AI-43346-08 and generous grants from Hoffman-La Roche Inc.,Wisconsin Alumni Research Foundation (WARF), and Shimadzu Scientific. MLF was partially supported by a PhRMA post-doctoral fellowship. CMR was partially supported by an AFPE gateway research fellowship.

REFERENCES

1. M. Constantinou, J. Y. Tsai, and H. Safran. Paclitaxel and concurrent radiation in upper gastrointestinal cancers. *Cancer. Investig.* **21**:887–896 (2003).
2. A. S. Retter, W. D. Figg, and W. L. Dahut. The combination of antiangiogenic and cytotoxic agents in the treatment of prostate cancer. *Clin. Prostate Cancer* **2**:153–159 (2003).
3. E. K. Rowinsky. Paclitaxel pharmacology and other tumor types. *Semin. Oncol.* **24**:S19-11–S19-12 (1997).
4. J. Treat, N. Damjanov, C. Huang, S. Zrada, A. Rahman. Liposomal-encapsulated chemotherapy: preliminary results of a phase I study of a novel liposomal paclitaxel. Oncology (Williston Park, NY. 15:44–48 (2001).
5. M. Socinski. Update on nanoparticle albumin-bound paclitaxel. *Clin. Adv. Hematol. Oncol.* **4**:745–746 (2006).
6. A. Sparreboom, S. D. Baker, and J. Verweij. Paclitaxel repackaged in an albumin-stabilized nanoparticle: handy or just a dandy? *J. Clin. Oncol.* **23**:7765-7767 (2005).
7. S. R. Croyand and G. S. Kwon. Polymeric micelles for drug delivery. *Curr. Pharm. Des.* **12**:4669-4684 (2006).
8. M. L. Forrest, C. Y. Won, A. W. Malick, and G. S. Kwon. *In vitro* release of the mTOR inhibitor rapamycin from poly(ethylene glycol)-*b*-poly(epsilon-caprolactone) micelles. *J. Control Release.* **110**:370–377 (2006).
9. M. L. Forrest, A. Zhao, C. Y. Won, A. W. Malick, and G. S. Kwon. Lipophilic prodrugs of Hsp90 inhibitor geldanamycin for nanoencapsulation in poly(ethylene glycol)-*b*-poly(epsilon-caprolactone) micelles. *J. Control. Release.* **116**:139–149 (2006).
10. J. A. Yanez, M. L. Forrest, Y. Ohgami, G. S. Kwon, N. M. Davies. Pharmacometrics and delivery of novel nanoformulated PEG-*b*-poly(epsilon-caprolactone) micelles of rapamycin. Cancer chemotherapy and pharmacology (2007).
11. H. M. Aliabadi, D. R. Brocks, and A. Lavasanifar. Polymeric micelles for the solubilization and delivery of cyclosporine A: pharmacokinetics and biodistribution. *Biomaterials.* **26**:7251–7259 (2005).
12. R. Vakiland and G. S. Kwon. PEG-phospholipid micelles for the delivery of amphotericin B. *J. Control. Release.* **101**:386–389 (2005).
13. R. Vakiland and G. S. Kwon. Poly(ethylene glycol)-*b*-poly (epsilon-caprolactone) and PEG-phospholipid form stable mixed micelles in aqueous media. *Langmuir.* **22**:9723–9729 (2006).
14. X. Shuai, T. Merdan, A. K. Schaper, F. Xi, and T. Kissel. Core-cross-linked polymeric micelles as paclitaxel carriers. *Bioconjug. Chem.* **15**:441–448 (2004).
15. J. Liu, Y. Xiao, and C. Allen. Polymer-drug compatibility: a guide to the development of delivery systems for the anticancer agent, ellipticine. *J. Pharm. Sci.* **93**:132–143 (2004).
16. S. Ali, I. Ahmad, A. Peters, G. Masters, S. Minchey, A. Janoff, and E. Mayhew. Hydrolyzable hydrophobic taxanes: synthesis and anti-cancer activities. *Anti-Cancer Drugs* **12**:117–128 (2001).
17. P. L. Soo, L. Luo, D. Maysinger, and A. Eisenberg. Incorporation and release of hydrophobic probes in biocompatible polycaprolactone-*block*-poly(ethylene oxide) micelles: Implications for drug delivery. *Langmuir.* **18**:9996–10004 (2002).
18. W. L. Klotz, M. R. Schure, and J. P. Foley. Determination of octanol-water partition coefficients of pesticides by microemulsion electrokinetic chromatography. *J. Chromatogr.* **930**:145–154 (2001).
19. S. Bai, S. M. Stepkowski, B. D. Kahan, and L. J. Brunner. Metabolic interaction between cyclosporine and sirolimus. *Transplantation.* **77**:1507–1512 (2004).
20. J. O'Brien, I. Wilson, T. Orton, and F. Pognan. Investigation of the Alamar Blue (resazurin) fluorescent dye for the assessment of mammalian cell cytotoxicity. *Eur. J. Biochem./ FEBS.* **267**:5421–5426 (2000).
21. A. B. Dhanikula, D. R. Singh, and R. Panchagnula. *In vivo* pharmacokinetic and tissue distribution studies in mice of alternative formulations for local and systemic delivery of

Paclitaxel: gel, film, prodrug, liposomes and micelles. *Curr. Drug Discov.* **2**:35–44 (2005).
22. P. Crosasso, M. Ceruti, P. Brusa, S. Arpicco, F. Dosio, and L. Cattel. Preparation, characterization and properties of sterically stabilized paclitaxel-containing liposomes. *J. Control. Release.* **63**:19–30 (2000).
23. J. A. Straub, D. E. Chickering, J. C. Lovely, H. Zhang, B. Shah, W. R. Waud, and H. Bernstein. Intravenous hydrophobic drug delivery: a porous particle formulation of paclitaxel (AI-850). *Pharm. Res.* **22**:347–355 (2005).
24. B. Davies and T. Morris. Physiological parameters in laboratory animals and humans. *Pharm. Res.* **10**:1093–1095 (1993).
25. P. Poulin, K. Schoenlein, and F. P. Theil. Prediction of adipose tissue: plasma partition coefficients for structurally unrelated drugs. *J. Pharm. Sci.* **90**:436–447 (2001).
26. L. van Zuylen, J. Verweij, and A. Sparreboom. Role of formulation vehicles in taxane pharmacology. *Invest. New Drugs.* **19**:125–141 (2001).
27. F. A. Greco, M. Thomas, and J. D. Hainsworth. One-hour paclitaxel infusions: review of safety and efficacy. *Cancer J. Sci. Am.* **5**:179–191 (1999).
28. E. K. Rowinsky. The taxanes: dosing and scheduling considerations. Oncology (Williston Park, NY. 11:7–19 (1997).
29. B. Nuijen, M. Bouma, J. H. Schellens, and J. H. Beijnen. Progress in the development of alternative pharmaceutical formulations of taxanes. *Invest. New Drugs.* **19**:143–153 (2001).
30. R. Pawar, A. Shikanov, B. Vaisman, and A.J. Domb. Intravenous and regional paclitaxel formulations. *Curr. Med. Chem.* **11**:397–402 (2004).
31. A. K. Singla, A. Garg, and D. Aggarwal. Paclitaxel and its formulations. *Int. J. Pharm.* **235**:179–192 (2002).
32. D. G. Rodrigues, D. A. Maria, D. C. Fernandes, C. J. Valduga, R. D. Couto, O. C. Ibanez, and R. C. Maranhao. Improvement of paclitaxel therapeutic index by derivatization and association to a cholesterol-rich microemulsion: *in vitro* and *in vivo* studies. *Cancer Chemother. Pharmacol.* **55**:565–576 (2005).
33. M. R. Dreher, W. Liu, C. R. Michelich, M. W. Dewhirst, F. Yuan, and A. Chilkoti. Tumor vascular permeability, accumulation, and penetration of macromolecular drug carriers. *J. Natl. Cancer Inst.* **98**:335–344 (2006).
34. S. C. Kim, D. W. Kim, Y. H. Shim, J. S. Bang, H. S. Oh, S. Wan Kim, and M. H. Seo. *In vivo* evaluation of polymeric micellar paclitaxel formulation: toxicity and efficacy. *J Control Release.* **72**:191–202 (2001).
35. C. Li, R. A. Newman, Q. P. Wu, S. Ke, W. Chen, T. Hutto, Z. Kan, M. D. Brannan, C. Charnsangavej, and S. Wallace. Biodistribution of paclitaxel and poly(L-glutamic acid)-paclitaxel conjugate in mice with ovarian OCa-1 tumor. *Cancer Chemother. Pharmacol.* **46**:416–422 (2000).
36. X. Zhang, H. M. Burt, G. Mangold, D. Dexter, D. Von Hoff, L. Mayer, and W. L. Hunter. Anti-tumor efficacy and biodistribution of intravenous polymeric micellar paclitaxel. *Anti-Cancer Drugs.* **8**:696–701 (1997).
37. E. Salvatorelli, P. Menna, S. Cascegna, G. Liberi, A. M. Calafiore, L. Gianni, and G. Minotti. Paclitaxel and docetaxel stimulation of doxorubicinol formation in the human heart: implications for cardiotoxicity of doxorubicin-taxane chemotherapies. *J Pharmacol. Exp. Ther.* **318**:424–433 (2006).